Flow Simulation in Abrasive Water Jet Machining of GFRP composite: The Effect of Operating Pressure and Standoff Distance on Kerf Width

Deepak D.,   **Anjaiah D.,**   **Yagnesh Sharma N** *

Manipal Institute of Technology,
Manipal University, Manipal- 576104, Karnataka state, India.

Abstract - **Abrasive Water Jet (AWJ) machining is a relatively new nontraditional machine tool used in machining of fiber reinforced composite. The quality of machined surface depends on various operating and material parameters. In the present work the effect of operating pressure and distance of the tool tip from target called the standoff distance (SOD) on AWJ characteristics is simulated using computational fluid dynamics (CFD). Computational domain was modeled based on experimental results of machining on Glass Fiber Reinforced Polymer (GFRP) composite. CFD results are compared with experimental output. The chosen parameters were found to have significant influence on the kerf width of work piece in AWJ machining. The effect on flow velocity in the domain is analyzed for the jet flow consisting of the mixture of garnet abrasives and water. It is found that distribution of jet velocity increases radially on work piece with the increase of SOD as well as operating pressure that result in widening of the kerf width on the work piece.**

Keywords— **Abrasive water jet machining, Jet velocity, GFRP composite, kerf width, operating pressure, standoff distance**

I.   Introduction

Abrasive Water Jet (AWJ) machining technology is evolving rapidly from the last decade. Manufacturing industry is becoming more time conscious and quality oriented with developing global economy. As a result the need for developing and understanding rapid manufacturing technology is ever increasing. These trends have forced the engineers to use advanced machining process like Electric Discharge Machining, Chemical Machining, Laser machining and AWJ machining for rapid production. The capability of machining of intricate shapes with good dimensional accuracy in hard, brittle and composite materials has made the AWJ machining process as an inevitable and one of the most popular non-conventional machining processes.

AWJ machining is an active field of research and scientists are working in various directions towards optimization of machining characteristics. Shimizu and Wu (2008) studied the effect of abrasive particle size on jet structure that was formed at exit of the nozzle using high speed photography. The effect of particle size (steel) on erosive wear of titanium alloy work piece was studied by Eltobgy et. al (2005) using three dimensional finite element analysis. Erosion rate was found to increase considerably for particle size up to 300 μm and remain constant for further increase of particle size. Similar trend was also observed by Yerramareddy et.al (1991). Deepak et al (2011, 2012) have found the effect of abrasive size and concentration in the flow on jet kinetic energy as well as on wall shear stress is marginal. Guihua Hu et.al (2008) investigated the effect of nozzle length on jet exit velocity using numerical technique and nozzle length was optimized to generate maximum jet velocity. Liu et al (2004) carried out computational Fluid Dynamics (CFD) analysis to study the jet dynamic characteristics of flow downstream. Tang P et.al (2009) investigated erosion pattern in slurry pipes using CFD. Deng Jianxin (2005) has made erosion study of boron carbide nozzle caused by abrasive particle impact by abrasive air-jets.

Comparative analysis of machining performance of garnet, aluminium oxide and silicon carbide on glass work piece was made by Khan et. al. (2007). Experimental investigations by Boud et. al. (2008), Gent et. al. (2008), Holmqvist et. al. (2008) summarizes garnet with size 80 mesh (180 μm) as optimal abrasive. Kantha Babu et. al. (2002) studied the effects of AWJ machining by using recycled abrasive. Lemma et. al. (2002) investigated the effects of jet oscillation on formation of striations on GFRP composite. Monno et. al. (2005) studied the effect of cutting head vibrations on structure of machined surfaces. Further Kantha Babu et. al. (2006) studied the surface roughness produced on aluminum alloys. The cut surface revealed the presence upper smoother zone, surface waviness at the middle and the lower part of work piece is characterized by the appearance of striations in curved pattern. A further study on the cause of striation on machined surface was made by Orbanic et. al (2008) using acrylic glass and aluminium samples. Azmir and Ahsan (2009)

*Corresponding author

Professor in the department of Mechanical and Manufacturing Engineering
Manipal Institute of Technology, Manipal University
Manipal- 576104, Karnataka state, India.
.

investigated the effect of process parameters on glass epoxy composite by experimental methods. In AWJ machining the quality of the machined surface depends on various process parameters such as abrasive hardness, shape, flow rate, operating pressure, SOD, jet impact angle, feed rate, nozzle diameter and target material properties. These parameters have influence on the energy distribution of the jet on the target materials. From the literature review it is understood that there is a scope for research that focus on application of numerical techniques to visualize the jet flow pattern that helps to explore a few aspects of material removal mechanism. In consideration of this aspect, the present work examines the effect of operating pressure and SOD on jet flow distribution on the target material. Detailed analysis of the jet structure that consists of mixture of garnet abrasives and water is made with respect to kerf width. The jet structure predicted by CFD analysis is compared with the actual kerf generated by experiments. It is found that the jet energy distribution increases radially on work piece with the increase of SOD and operating pressure.

Nomenclature

d_p	Diameter of abrasive particles (μm)
F_{Lift}	Lift force (N)
F_s	External body force (N)
F_{vm}	Virtual mass force (N)
G_k	Turbulent kinetic energy due to velocity gradient
G_b	Turbulent kinetic energy due to buoyancy
K	Momentum exchange co-efficient
l	Length of flow domain (mm)
L	Particle spacing (mm)
$\dot{m}$	Mass flow rate of mixture (m³/s)
S_k	User defined source terms
t_s	system response time (s)
V	Velocity of phase (m/s)
Y_M	Contribution fluctuating dilation
α	Volume fraction of the phase
ρ	Density of suspension mixture (kg/m³)
γ	Density ratio
$C_{1\varepsilon}, C_{2\varepsilon}, C_{3\varepsilon}$	Constants
τ_d	Particle response time (s)
μ	Viscosity (kg/m-s)

II.   Theoretical formulation

A.   *Numerical Model and Assumptions*

The numerical region for flow analysis is made up of flow geometry as shown in the figure 1. Computational domain consists of nozzle with inlet diameter and length of converging section 4 mm, focus tube of diameter 0.8 mm and length 17 mm. The mixture Abrasive and water is let into the nozzle at the inlet and is carried down through the converging cone to the focus tube and exits as coherent jet at the nozzle exit. Further in front of the nozzle the computatonal domain is modeled to capture the flow characteristics of the jet when it

pierces through the GFRP laminate of 3 mm thickness at various SOD and operating pressure as mentioned in table 1. The following assumptions were made in the present work.

- Flow is considered to be two-phase flow
- The primary phase is liquid phase which is continuous and incompressible.
- The secondary phase is a solid phase that consists of homogeneously mixed garnet abrasives of equal diameter.
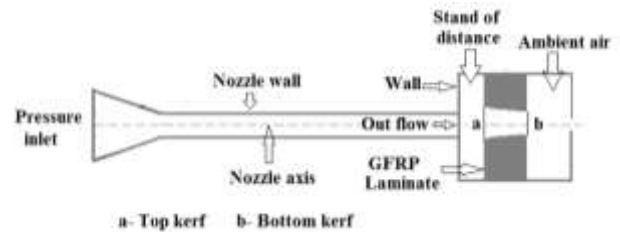- Two-phase flow assumed is steady and characterized by turbulent flow.

Fig.1. Computational model of AWJ Machining process

B.   *Selection of multiphase model*

There are three multiphase models namely, VOF, Mixture and Eulerian model. Ideal model for numerical simulation depends on Particulate loading (*β*) and the Stokes number (S_t).

$$\beta = \frac{\alpha_s \rho_s}{\alpha_l \rho_l} \qquad (1)$$

$$\tau_d = \frac{\rho_d d_d^2}{18\mu_l} = 5.05129\,x10^{-4} \quad (2)$$

$$t_s = \frac{l}{v} = 1.4218\,x10^{-3} \qquad (3)$$

$$S_t = \frac{\tau_d}{t_s} = 0.3552 \qquad (4)$$

The Particulate loading for garnet abrasive is 0.230 and hence degree of interaction between the phases is intermediate loading, the coupling is two-way. For Stokes number less than one, particles will closely follow the fluid flow. All mentioned multiphase models can handle this type of problem, the Eulerian multiphase model seems to be the most accurate one (Fluent, 1998). Present numerical simulation is carried using Eulerian multiphase model embedded in Fluent software.

The governing equations for mass and momentum conservation are solved for the steady incompressible flow. The coupling between velocity and pressure has been attempted through the phase coupled SIMPLE algorithm developed by Patankar (1972) using the first order upwind scheme for the solution. The turbulence is modeled using standard k-ε turbulence model. The governing partial differential equations for mass and momentum conservations are detailed below.

Continuity Equation

$$\frac{1}{\rho_{pq}}\left[\frac{\partial}{\partial t}(\alpha_q\rho_q)+\nabla\bullet(\alpha_q\rho_q v_q)\right]=\sum_{p=1}^{N}(m_{pq}-m_{qp}) \quad (5)$$

The conservation of momentum equation (solid phase)

$$\frac{\partial}{\partial t}(\alpha_s\rho_s v_s)+\nabla\bullet(\alpha_s\rho_s v^2_s)=-\alpha_s\nabla p-\nabla p_s +$$

$$\nabla\bullet\tau_s+\alpha_s\rho_s g+\sum_{l=1}^{N}\left[k_{ls}(v_l-v_s)+(m_{ls}v_{ls}-m_{sl}v_{sl})\right]$$

$$+(F_s+F_{lift,s}+F_{vm,s}) \quad (6)$$

The conservation of momentum equation (fluid phase)

$$\frac{\partial}{\partial t}(\alpha_q\rho_q v_q)+\nabla\bullet(\alpha_q\rho_q v^2_q)=-\alpha_q\nabla p+\nabla\bullet\tau_q +$$

$$\alpha_q\rho_s g+\sum_{p=1}^{N}\left[k_{pq}(v_p-v_q)+(m_{pq}v_{pq}-m_{qp}v_{qp})\right]$$

$$+(F_q+F_{lift,q}+F_{vm,q}) \quad (7)$$

III. Method of solution

A. *Numerical Scheme*

Conservation equations are solved for each control volume to obtain the velocity and pressure fields. Convergence is effected when all the dependent variable residuals fall below $1E^{-5}$ at all grid points. Computational domain is modeled using commercially available pre-processor routine called GAMBIT and meshing is carried out using linear quad paved mesh. Wall region in the flow domain is closely meshed using the boundary layer mesh concepts for extracting high velocity gradients near the boundary walls. According to the structure of nozzle and jet characteristics, computational domain is built as axi-symmetric model. Figure 2 shows the computational domain of complete model. The grid independence test is performed to check the quality of mesh for solution convergence. Mesh geometries consisting of 10660, 17862, 19786, 22859, 25194, 29172, 39920, 46176 and 61568 quadrilateral cells were build and nozzle exit velocity is calculated. Further refining mesh size did not bring variation in axial velocity by more than 1.2 %. By considering lesser computational time required, a mesh geometry consisting of 29172 control volumes has been adopted in this work.
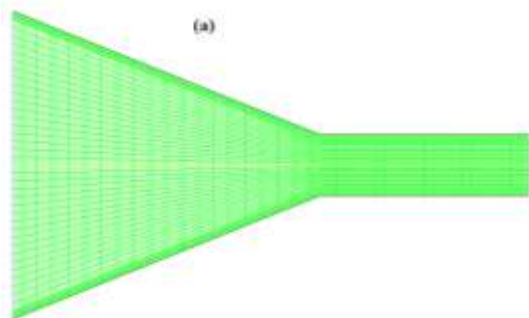

Fig. 2 A portion of the meshed domain near the critical section of AWJ nozzle

B. *Boundary and Operating Conditions*

Boundary conditions are imposed on the computational domain, as per the physics of the problem. Inlet boundary condition is specified by the operating pressure entering the nozzle. It is assumed that pressure at inlet is uniform across the cross section. At the exit, static pressure of effluxing flow is taken to be zero (gauge), so that the computation would proceed by the relative pressure differences across the grid volumes for the entire domain of the flow. Wall boundary conditions are impressed to bound fluid and solid regions on nozzle inside as well as on target work piece. In viscous flow models, as in the present case, velocity components at the wall are set to zero in accordance with the no-slip and impermeability conditions that exist on the wall boundary. The axis of the nozzle is used to solve the computational domain as axisymmetric problem i.e., the gradient of fluid properties are set to zero across the axis line.

TABLE 1 NUMERICAL SIMULATION PARAMETERS

Numerical simulation parameters	
Operating parameter	Input values
Inlet pressure (MPa)	90, 120, 150
Standoff distance (mm)	1, 3, 5
Constant parameters	
Average size of the garnet	180 micron
Concentration of abrasive	6 %
Density of water	1000 Kg/m^3
Density of garnet	2300 Kg/m^3

IV. Results and Discussion

A. *Validation of the numerical model*

Validation of the numerical simulation was made with the velocity profiles of jet flow in AWJ nozzle as obtained Gua et al (2008) for the purpose of numerical calibration of the computational scheme. Velocity distribution is generated along the axis of the nozzle with input velocity of 25.6 m/s and the obtained profile is overlapped with the velocity distribution obtained by Gua et al for the purpose of comparsion. It is seen from the figure 3 that velocity profiles obtained in the present work agrees well with the cited reference.
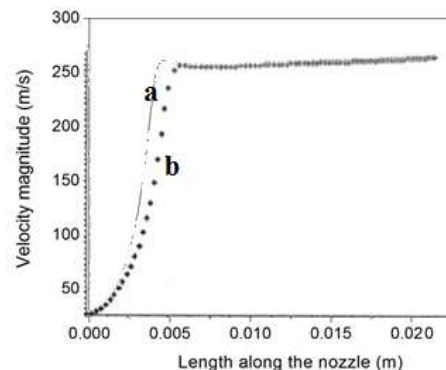

Fig 3. The velocity distribution : a- velocity profile reproduced in the present work as against the velocity profile obtained by Gua et al

International Journal of Advancements in Mechanical and Aeronautical Engineering– IJAMAE
Volume 1: Issue 2   [ISSN 2372-4153]

Publication Date : 25 June 2014

B. *The effect of operating pressure on kerf width*

Numerical simulation was carried out to capture the flow characteristics at operating pressures of 90, 120 and 150MPa. The SOD and abrasive concentration in water were maintained constant at 1mm and 6% respectively in all simulations. Figure 4 shows the radial distribution of the jet velocity on the top kerf width at chosen pressures. It is seen from figure 4 that the maximum axial jet velocity is at the center of the nozzle and it gradually decreases radially after a distance of about 0.35 mm from the center. Similar trend is followed at all operating pressures in the simulation. Also it is observed that with the increase of operating pressure, the axial velocity at the center of the nozzle increases significantly but marginally increases in the radial direction. The radial increase of jet velocity is mainly due to increase in the turbulence that causes jet expansion. This leads to an increase in kerf width on the cut surface and the effect is relatively more at higher pressures. The effect of pressure on kerf width is compared with the kerf width generated on GFRP composite by experiments at similar operating conditions (fig 5). It is seen that there is a close agreement of kerf width produced in each case.
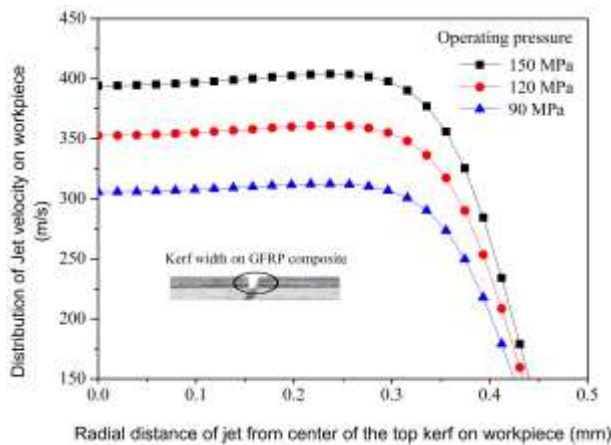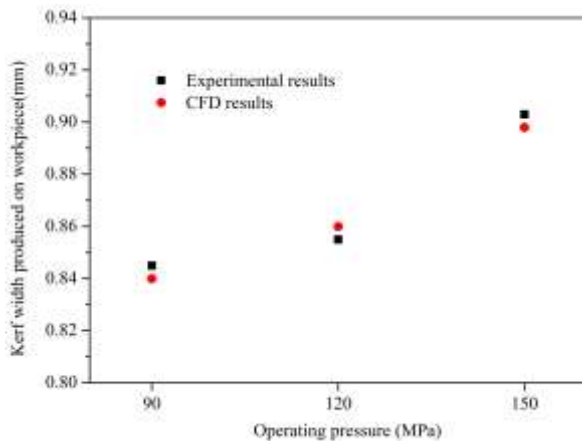
C. *The effect of standoff distance on kerf width*

Standoff distance i.e., the distance between target and nozzle exit was kept at 1, 3 and 5 mm to study its effect on kerf width produced due to jet expansion. Operating pressure and abrasive concentration was kept constant in simulations. Figure 6 shows the axial velocity plots at different SOD. It is observed from the figure that the axial velocity decreases along the axis of the nozzle towards the work piece which is clearly shown in figure 8 through the contour plots. The jet diameter is smaller at SOD corresponding to 1 mm and it increase to a maximum at SOD of 5 mm as shown in figure 6. This happens mainly due unrestricted jet disintegration due to flow turbulence. It is also seen from the figure 6 that as the jet diameter increases, it losses its axial velocity. The CFD results were compared with kerf width obtained during the experimental study (Fig. 7) and error in kerf width predicted was found to be 4 % of the actual. Also it is seen from the contour plots that, as the jet traverses in air or through the material, it loses its energy and thereby machining capability. Thus it produces wider kerf at the entry than at the exit at any operating condition.
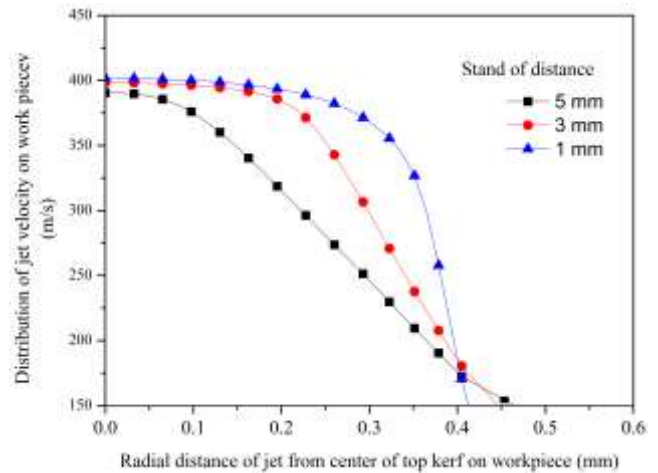
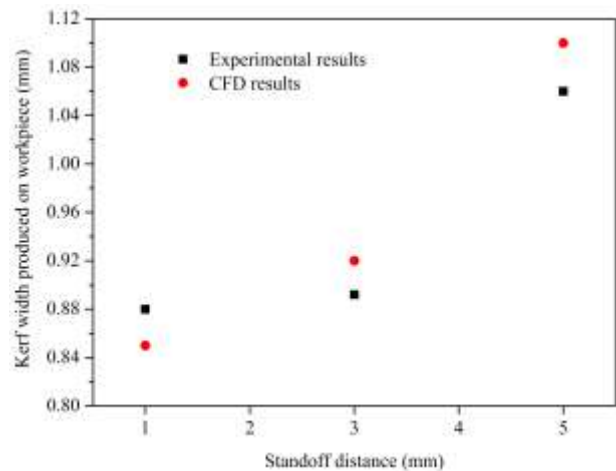Fig 4. Plot of jet velocity distribution on workpiece at various pressures

Fig 6. Plot of jet velocity distribution on workpiece at various SOD

Fig 5. The kerf width on workpiece at various pressures

Fig 7. The kerf width on workpiece at various pressures

International Journal of Advancements in Mechanical and Aeronautical Engineering– IJAMAE
Volume 1: Issue 2   *[ISSN 2372-4153]*
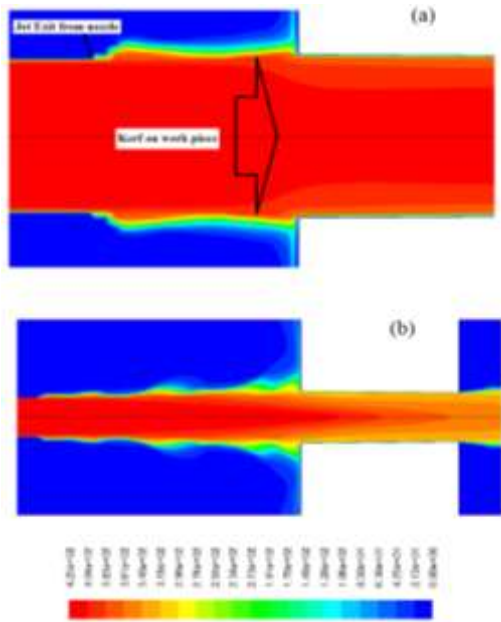
Publication Date : 25 June 2014

Fig 8. Countour plot of jet velocity distribution on workpiece

V.   Conclusions

Following major conclusions can be drawn from the present numerical investigation.

- The operating pressure increases the jet velocity on work piece and thus the impact force. Though penetrating capability of the jet is superior at higher operating pressures, it generates wider kerf on the work piece due to jet expansion.

- The SOD has direct influence on jet diameter which increases with increase in SOD. Wider kerfs are produced on work piece at relatively larger SOD. Also higher SOD results in decreased jet velocity. Hence to maintain good machining capability of AWJ, lower SOD must be chosen.

Acknowledgment

References

[1]   Azmir, M., Ahsan, A. K., 2009. Study of abrasive water jet machining process on glass/epoxy composite laminate. Journal of Materials Processing Technology 209 (20), pp. 6168-6173

[2]   Boud, F., Carpenter, C., Folkes, J., Shipway, P. H., 2010, Abrasive waterjet cutting of a titanium alloy: The influence of abrasive morphology. Journal of Materials Processing Technology 210 (15), pp. 2197-2205.

[3]   Deepak. D, D. Anjaiah, N. Yagnesh Sharma, 2011, Numerical analysis of flow through abrasive water suspension jet: The effect of abrasive grain size and jet diameter ratio on wall shear, International Journal of Earth Sciences and Engineering, Vol - 04, pp. 78-83.

[4]   Deepak, D., Anjaiah, D., Vasudeva Karanth, K., 2012, Yagnesh Sharma, N., 2012. CFD simulation of flow in an abrasive water suspension jet the effect of inlet operating pressure and volume fraction on skin friction and exit kinetic energy, Advances in Mechanical Engineering , doi:10.1155/2012/186430

[5]   Eltobgy, Elbestawi, 2005. Finite element modeling of erosive wear. International Journal of Machine Tools & Manufacture 45, pp.1337-1346

[6]   Fluent User's Guide, vol. 3, Fluent Incorporated Publishers, Lebanon, 1998.

[7]   Ghu, W. Zhu, T. Yu, and J. Yuan, Numerical Simulation and Experimental Study of Liquid-solid Two-phase Flow in Nozzle of DIA Jet, Proceedings of the IEEE Intl. conference industrial informatics(INDIN 2008), Daejeon, Korea, July 13-16th 2008.

[8]   Gent M., Menendez , Torno S, Schenk A., Orientative deformation mode cutting results of some alternative abrasives for applications in abrasive waterjet cutting, In: Proceedings of the 19th International Conference on Water Jetting, Nottingham Univ., UK, 15–17 Oct 2008, pp. 289–303.

[9]   Jianxin Deng, 2006, Sand Erosion Performance of Gradient Ceramic Nozzles by Abrasive Air-Jets, ASME 2006 International Manufacturing Science and Engineering Conference Manufacturing Science and Engineering, Parts A and B, pp. 455-459.

[10] Holmqvist, G., Honsberg, U., 2008. Sensitivity analysis of abrasive waterjet cutting economy. In: Proc. 19th International Conference on Water Jetting, Nottingham Univ., UK, 15–17 Octr 2008, pp. 273–287

[11] Khan A. A., Haque, M. M., 2007, Performance of different abrasive materials during AWJ machining of glass. Journal of Materials Processing Technology 191, pp. 404–407

[12] Kantha Babu, M. O., Krishnaiah Chetty, V., 2003. Studies on recharging of abrasives in abrasive water jet machining. Wear 254, pp. 763–773

[13] Liu, H. et al., 2004. A study of abrasive waterjet characteristics by CFD simulation. Distribution, 154, pp.488–493.

[14] Monno M. & Ravasio C., 2005, The effect of cutting head vibrations on the surfaces generated by waterjet cutting", International Journal of Machine Tools and Manufacture, vol. 45(3), pp.355–363.

[15] Orbanic, H. & Junkar, M., 2008. Analysis of striation formation mechanism in abrasive water jet cutting. Wear, 265, pp.821–830.

[16] S. V. Patankar and D. B. Spalding, 1972, A calculation procedure for heat, mass and momentum transfer in three-dimensional parabolic flows," International Journal of Heat and Mass Transfer, vol. 15, no. 10, pp. 1787–1806.

[17] Z. Shangxian, L. Yan, W. Quan, B. Discretization, and G. Space, Track Calculation and Numerical Simulation on Particles in High Pressure Abrasive Water Jet Nozzle, IEEE Intl. Conf. on Measuring Technology and Mechatronics Automation 2010, pp. 1039-1042.

[18] Shimizu, Z., Shinoda, Y., Peng, G., 2008. Flow characteristics of water jet issuing from a fan jet nozzle. In proceedings of 19th International conf. on water jetting, Nottingham, UK, 15th -17th Oct, 2008, pp. 55-66

[19] P. Tang, J. Yang, J. Y. Zheng et al, 2009, Erosion-corrosion failure of REAC pipes under multiphase flow," Frontiers of Energy and Power Engineering in China, vol. 3, no. 4, pp. 389–395.

[20] Yerramareddy, Bahadur, 1991. Effect of operational variables, microstructure & mechanical properties on the erosion of Ti–6Al–4V, Wear 142, pp.253–263.

[21] Lemma, E. et al., 2002. Study of cutting fiber-reinforced composites by using abrasive water-jet with cutting head oscillation. *Composite Structures*, 57, pp.297–303.